

“Effects of Ozone Depletion on Aquatic Ecosystems”

D.-P.-Häder, ed., submitted 10 May 1996; revised September 1996; accepted for publication

Biological Weighting Functions for Describing the Effects of Ultraviolet Radiation on Aquatic Systems

John J. Cullen

Center for Environmental Observation Technology and Research
Department of Oceanography
Dalhousie University
Halifax, Nova Scotia, B3H 4J1, Canada

Patrick J. Neale

Smithsonian Environmental Research Center
P.O. Box 28
Edgewater, Maryland, 21037, USA

Introduction

In order to evaluate the effects of ultraviolet radiation (UV; 280 - 400 nm) on aquatic ecosystems, and to predict the potential influence of enhanced ultraviolet-B radiation (UV-B; 280 - 320 nm)[†] from ozone depletion, it is necessary to observe the effects of natural and experimentally-altered UV on different biological and chemical systems, and to quantify measured responses as functions of irradiance and time. Because biological and chemical effects of UV are strongly dependent on wavelength, spectral weighting functions must be applied to relate experimental responses quantitatively to UV exposure, if the results are to have any use for predicting effects in nature.¹⁻⁴ This is reality, not opinion. The fact is that if any biological or chemical effect is expressed as a function of radiant exposure for regimes with different spectral irradiance (i.e., different depths in the water column, times of day or year, or different artificial sources of UV), a weighting function is used, either explicitly or implicitly. An appropriate weighting function must be applied, therefore, or at least the uncertainties associated with the chosen weighting function should

[†] The Commission Internationale de l'Éclairage (CIE) defines UV-B as 280 - 315 nm and ultraviolet-A (UV-A) as 315 - 400 nm. Here, we will follow the preference of many aquatic scientists and accept 320 nm as the boundary between UV-B and UV-A. With respect to biological processes, there are no consistent discontinuities in response at either 315 nm or 320 nm.

be appreciated. Instead of reviewing the development of operating principles (reviewed in refs. 1-7), we will illustrate them with real data and results of model calculations.

We discuss spectral weighting functions (SWFs) in general and biological weighting functions (BWFs) in particular. In the past, BWFs were called action spectra.¹⁻³ Subsequently, the terms have been used interchangeably. There are, however, important differences between action spectra and BWFs that can and should be identified. We propose that “action spectrum” should be applied to SWFs that are determined through experimental exposures of samples to monochromatic radiation at different wavelengths (because interactions between wavelengths are unimportant);³ the term “biological weighting function” should be reserved for SWFs that are determined through polychromatic exposures,^{1,2} in explicit recognition of the interactions between wavelengths that characterize complex biological responses to UV. We will focus on biological responses to UV (particularly the inhibition of photosynthesis) because the interactions between wavelengths and the potential for time-dependence make them much more complicated (but not necessarily more ecologically important) than many photochemical processes that can be characterized by action spectra.

Quantifying Radiant Exposure

When algal photosynthesis (P) is described as a function of irradiance, exposure is often measured and expressed as photosynthetically available radiation (PAR; 400 - 700 nm, W m^{-2} or $\mu\text{mol quanta m}^{-2} \text{s}^{-1}$). A crude spectral weighting function is used to quantify effective irradiance: wavelengths < 400 nm and > 700 nm are excluded because utilization of those wavelengths for photosynthesis is considered to be negligible. Consequently, P vs. PAR relationships are justifiably insensitive to variability in near-infrared relative to PAR. It is well recognized, however, that PAR is not the best measure of the irradiance available for aquatic photosynthesis: for most algal assemblages, blue and red wavelengths are utilized much more efficiently than green wavelengths, but the ratios of those wavebands vary with solar angle and atmospheric conditions, and they change with depth in the water column.⁸ It is thus useful to weight spectral irradiance with a function describing the spectral response of algal photosynthesis, thereby quantifying photosynthetically utilizable radiation (PUR).⁹ Nonetheless, it is common to see aquatic photosynthesis described as a function of PAR. If both P and PAR are measured in situ, the relationships between P and PAR are accurate, but not directly applicable to other environments where ratios of PUR:PAR might be different. If P vs PAR is measured in incubators that attenuate light with neutral density screens (i.e., the ratio of PUR:PAR is relatively constant in the incubator),

application to natural water columns can be biased¹⁰ to the extent that PUR:PAR is different in nature and variable with depth.¹¹

The important points are: 1) A relatively crude weighting function (PAR) can be used to quantify irradiance available for photosynthesis — it excludes wavelengths that we know are generally unimportant in nature; and 2) The PAR weighting function is insensitive to spectral variability within the 400 - 700 nm waveband, and thus PAR alone cannot be used to predict important modes of variation in photosynthetic efficiency with location and depth.

A comparable situation exists with respect to biological responses to UV. Numerous effects have been quantified as functions of broad-band measures of UV (i.e., UV-B and/or UV-A), and a few have been characterized with spectral weighting functions. However, there is little appreciation of how much predictability a researcher sacrifices by quantifying a biological response as a function of some broad-band measure of UV, rather than as a function of appropriately weighted radiant exposure. We will explore some of the consequences here.

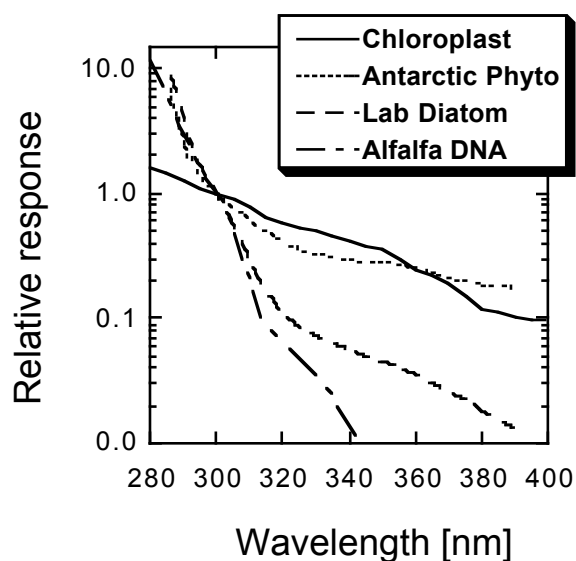


Figure 1. Biological weighting functions. For this comparison, relative response has been normalized to 1.0 at 300 nm: (—) inhibition of partial photosynthetic reactions in chloroplasts;¹² (···) inhibition of photosynthesis during 60-min incubations of natural Antarctic phytoplankton grown in outdoor culture (ref.13, in which incubation time was mistakenly reported as 30 min); (---) inhibition of photosynthesis during 45-min incubations of the diatom *Phaeodactylum* in culture;¹⁴ and (— · —) the action spectrum for pyrimidine dimer induction in alfalfa seedlings.¹⁵

Biological Weighting Functions

To quantify biologically effective irradiance (E^* , dimensionless), photon fluence at each wavelength ($E(\lambda)$; $\text{W m}^{-2} \text{nm}^{-1}$) must be weighted according to its biological effectiveness ($W(\lambda)$; $(\text{W m}^{-2})^{-1}$):^{2,3,14,16,17}

$$E^* = \int_{\lambda=280 \text{ nm}}^{700 \text{ nm}} W(\lambda) \cdot E(\lambda) \cdot d\lambda \quad (1).$$

The coefficients, $W(\lambda)$, constitute a BWF. An alternative approach is to define weighted irradiance, E_{Beff} , with units $(\text{W m}^{-2})_{\text{Beff}}$, in which case the coefficients, $W(\lambda)$, are dimensionless. The critical requirement, and the raison d'être for a BWF, is that it quantifies the relevant radiant exposure so that the effect of the exposure is a function of E^* (or E_{Beff}), regardless of the shape of the irradiance

spectrum.¹⁸ We choose to determine dimensionless E^* because it directly quantifies the effect if the form of the response function is known (i.e., if UV irradiance reduces photosynthesis proportional to $1/(1 + E^*)$,¹⁴ then $E^* = 1$ corresponds to 50% inhibition). Functions that are normalized (e.g., to 1.0 at 300 nm; Fig. 1) can predict *relative* changes in the biological effect as a function of changes in spectral irradiance, but the absolute magnitude of the biological effect can be calculated only if it is quantified for at least one biologically weighted radiant exposure.

The key role of BWFs has been well described in several papers that should be required reading for anyone interested in quantifying the biological effects of UV.^{1-3,18} Spectral weighting functions have been determined for many processes,¹⁹ such as damage to DNA,^{15,16} inhibition of motility in an alga,²⁰ inhibition of photosynthesis in higher plants,^{1,2} and in marine phytoplankton.^{13,14,21-24} The spectra have different shapes (Fig. 1), and many extend well into the UV-A (320 - 400 nm). Clearly, neither a measurement of UV-B nor irradiance weighted by any one SWF can quantify accurately the influence of environmental radiation on different biological processes.

The Importance of a Good Weighting Function

Weighted irradiance spectra show which wavelengths are most biologically effective, and comparisons between spectra emphasize the key wavebands (Fig. 2). If the wrong weighting function is used to quantify irradiance, then comparisons between radiant exposures are compromised.¹⁸ For example, if one considers damage to DNA in alfalfa,¹⁵ a 50% depletion of ozone corresponds to a 57% increase in biological damage (example in Fig. 2B). If biologically effective irradiance for inhibiting photosynthesis in a diatom is considered,¹⁴ the relative increase is estimated to be 24% (Fig. 2C), whereas a broad-band UV-B meter (Fig. 3) might report an increase of 146% associated with the same ozone depletion (Fig. 2D). These comparisons demonstrate that if the weighting function for a biological process is not known, the biological effect associated with a change in spectral irradiance is uncertain at best. This uncertainty might be a big problem, because appropriate weighting functions are not known for many biological responses, and also because many researchers are able to quantify irradiance only with an inexpensive, broad-band meter that in practice applies a weighting function determined solely by its spectral sensitivity (Fig. 3).

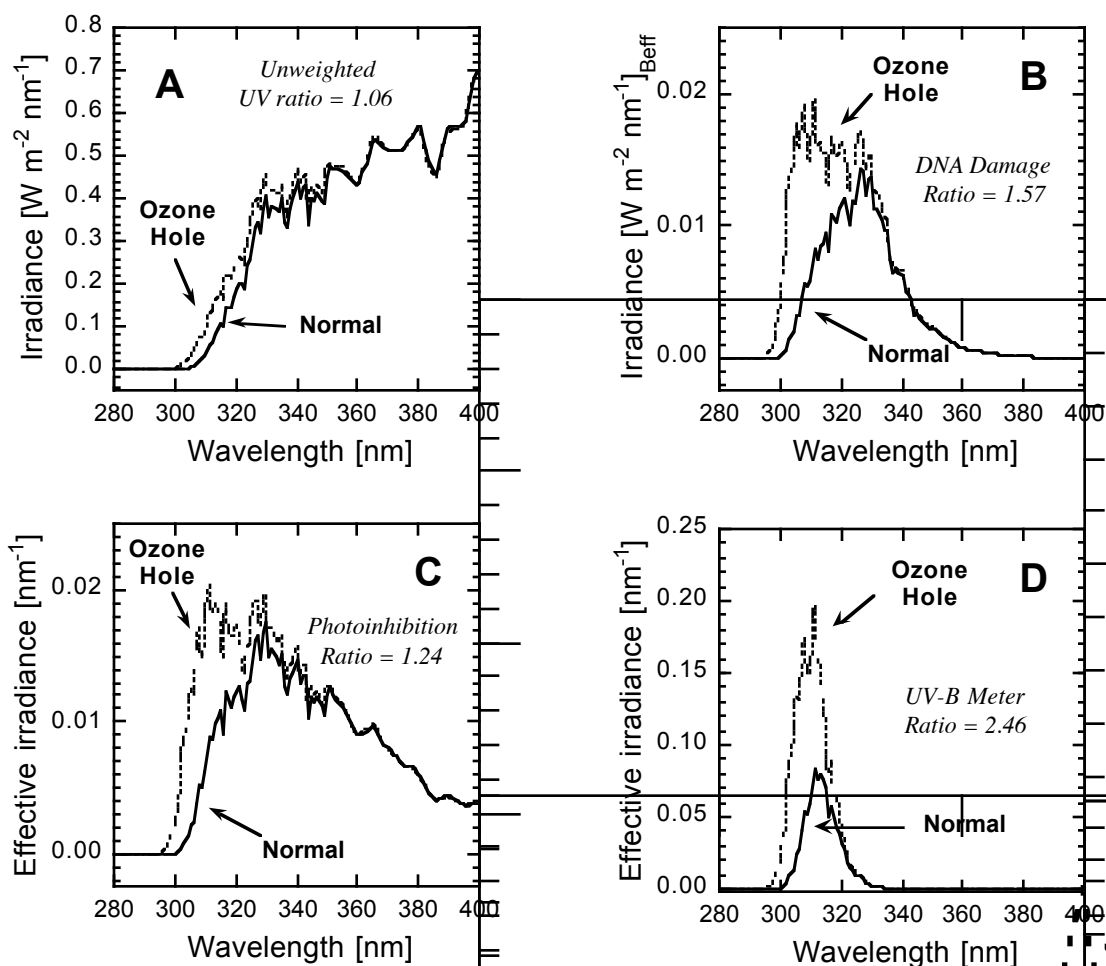


Figure 2. The calculated effects of ca. 50% ozone depletion associated with the Antarctic Ozone Hole. A) Measurements of solar irradiance²⁵ were made at McMurdo Station, Antarctica (78°S) on 28 October 1990 (Ozone Hole, 175 Dobson Units [DU]) and 10 November 1990 (Normal, 350 DU). To correct for cloud cover, the spectrum from 28 October was multiplied by a factor of 1.53 to match that of 10 November for integrated irradiance, 350 - 400 nm; B) the same measurements, weighted by the spectrum for DNA damage in alfalfa seedlings¹⁵ normalized to 1.0 at 300 nm; C) weighted by the BWF for inhibition of photosynthesis in *Phaeodactylum*;¹⁴ and D) weighted by the response of a hypothetical broad-band UV-B meter (see Fig. 3). Relative increases in weighted irradiance (unweighted UV, $W m^{-2}$, in A) associated with ozone depletion are reported as ratios for each measure. Note that the weighted irradiance spectra show what the biological or radiometric system “sees” and integrates (see ref. 1).

How important is the spectral weighting? In some cases, inappropriate representation of biologically effective irradiance can lead to big errors in the prediction of UV effects in nature. To explore the influence of spectral weighting on the quantification of biologically effective UV, we have prepared a rather intricate and perhaps intimidating comparison (Table 1). We will discuss subsets of the data to illustrate important principles of environmental radiometry.

Table 1. Different measures of UV radiation. The modeled spectra are from a clear-sky solar irradiance model.²⁶ Midday spectra at 45°N and the equator are simulated for 300 Dobson Units (DU: 10^3 cm O₃) at the equinox; spectra for 60°S are for high O₃ (340 DU) and low O₃ (140 DU) during the austral spring. Effects of clouds on low- O₃ spectra are approximated with a 40% reduction at all wavelengths. Irradiance at 5 m is estimated using diffuse attenuation coefficients (m⁻¹) measured in the Weddell-Scotia Sea.²⁷ Direct measurements of solar irradiance at McMurdo Station, Antarctica (78°S) are the same as in Fig. 2. Spectra from sunlamps, unfiltered and filtered through cellulose acetate, are from a laboratory study.²⁸ In the upper panel, unweighted UVB ($W\ m^{-2}$) and readings from a hypothetical UVB meter (Fig. 3) are reported in $W\ m^{-2}$. Weighted irradiance [$(W\ m^{-2})_{\text{Bref}}$] for the Setlow DNA action spectrum,¹⁶ alfalfa DNA spectrum (converted to energy units),¹⁵ and a spectrum for photoinhibition of partial reactions in chloroplasts¹² come from spectra normalized to 1.0 at 300 nm. The weighting functions for photoinhibition in *Phaeodactylum*¹⁴ and for outdoor cultures of natural Antarctic phytoplankton¹³ are in units of $(W\ m^{-2})^{-1}$; thus biologically weighted irradiance (E^*) is dimensionless: the reduction of photosynthesis due to photoinhibition is $(1/(1 + E^*))$. To illustrate how the comparison of different exposures is sensitive to the weighting function, each measure in the lower panel is normalized to that modeled for 45°N. In the text, elements of this table are identified by row and column, i.e., K9 = 2.86.

	Modeled Spectra					Measured Spectra				Row	
	45°N	Equator	60°S high O ₃	60°S low O ₃	60°S low O ₃ x 0.6	60°S low O ₃ 5 m	McMurdo Normal O ₃	O ₃ hole	Laboratory Bare lamp		Filtered lamp
UVB	1.62	3.30	1.42	2.44	1.46	0.44	1.27	2.31	1.61	0.31	A
UVB Meter	1.62	3.86	1.33	3.46	2.07	0.56	1.00	2.46	4.90	0.74	B
Setlow DNA	0.046	0.161	0.032	0.232	0.139	0.032	0.016	0.077	2.129	0.175	C
Alfalfa DNA	0.45	0.92	0.40	0.72	0.43	0.14	0.39	0.62	1.28	0.15	D
Chloroplast	9.40	16.11	9.03	9.97	5.98	2.97	9.93	11.22	1.75	0.40	E
<i>Phaeodactylum</i>	0.89	1.61	0.84	1.09	0.65	0.29	0.89	1.10	0.96	0.12	F
Antarctic phyto	0.98	1.67	0.95	1.03	0.62	0.33	1.03	1.14	0.20	0.04	G
	Relative to 45°N										
UVB	1.00	2.04	0.88	1.51	0.91	0.27	0.78	1.43	0.99	0.19	H
UVB Meter	1.00	2.39	0.82	2.14	1.28	0.34	0.62	1.52	3.03	0.46	I
Setlow DNA	1.00	3.53	0.69	5.07	3.04	0.71	0.35	1.68	46.62	3.83	J
Alfalfa DNA	1.00	2.05	0.90	1.62	0.97	0.31	0.88	1.37	2.86	0.34	K
Chloroplast	1.00	1.71	0.96	1.06	0.64	0.32	1.06	1.19	0.19	0.04	L
<i>Phaeodactylum</i>	1.00	1.81	0.94	1.22	0.73	0.32	1.00	1.24	1.08	0.13	M
Antarctic phyto	1.00	1.70	0.96	1.05	0.63	0.34	1.05	1.16	0.21	0.04	N
Column	1	2	3	4	5	6	7	8	9	10	

Ultraviolet-B as a measure of biologically damaging irradiance. When a relevant BWF is unavailable, it would seem appropriate to express a measured biological effect as a function of unweighted UV,²⁹ or UV-B and UV-A considered separately.³⁰ Exposure to UV-B can be measured accurately with a scanning spectroradiometer,^{25,30} or calculated from a solar radiation model.^{26,31-33} By relating a biological effect quantitatively to UV-B (W m^{-2}), a biological weighting function is applied, with a relative weight of 1.0 for 280 - 320 nm, and a weight of zero for other wavelengths. Is this an acceptable simplification?

In the lower panel of Table 1, different measures of damaging irradiance are normalized to the value for clear-sky midday solar irradiance at 45° latitude at the equinox (“mid-latitude standard”; Table 1, column 1). If unweighted UV-B (W m^{-2}) is a good measure of biologically effective irradiance for a particular process, then UV-B, relative to the mid-latitude standard, would be nearly the same as appropriately weighted irradiance, relative to the same standard exposure. For the comparisons presented here, unweighted UV-B (row H) is indeed a good measure of DNA-damaging solar irradiance (row K), if one accepts a recently published action spectrum for dimer induction in the DNA of alfalfa seedlings.¹⁵ However, the close correspondence between UV-B (W m^{-2}) and DNA-damaging irradiance ($\text{W m}^{-2}_{\text{Beff}}$) does not extend to comparisons between artificial sources and solar irradiance: an unfiltered sunlamp providing UV-B fluence essentially equal to 45° latitude at noon (H9) would damage DNA 2.86 times as effectively than the mid-latitude standard exposure (K9). A similar lamp, filtered with cellulose acetate to exclude shorter wavelengths, would emit 19% the UV-B of the mid-latitude standard (H10), but it would be 34% as damaging to alfalfa DNA (K10). An experimenter who uses UV-B fluence to relate sunlamp exposures to natural solar irradiance would thus overestimate DNA damage in nature when extrapolating laboratory results. Consequently, commonly used laboratory exposures, quantified as unweighted UV-B, cannot be related accurately to solar irradiance in nature.

Table 1 indicates that for natural exposures in surface waters near midday, unweighted UV-B, relative to a mid-latitude standard, would be a reasonably good measure of damaging irradiance with respect to effects on DNA in a higher plant,¹⁵ but UV-B does not serve as well for representing biological effectiveness according to other weighting functions. Thus, if the weighting function for a biological process is unknown, one cannot expect the biological effect to be a consistent function of UV-B. Indeed, irregularities in the relationship between biological effect and weighted irradiance can be used as a diagnostic of an inappropriate BWF.¹⁸

Broad-band measures of UV-B. Ultraviolet-B irradiance is commonly measured with a broad-band radiometer that applies its own weighting function according to its spectral response (Fig. 3).

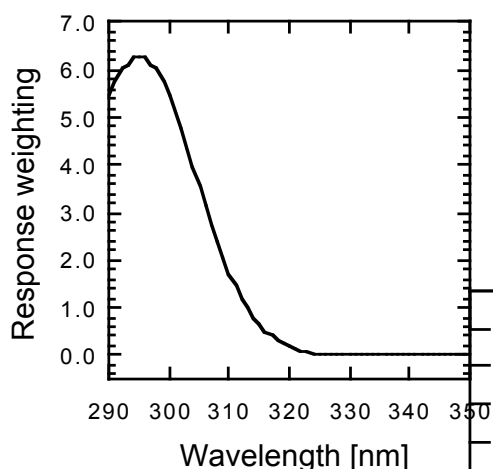


Fig. 3. The response (dimensionless weightings, yielding a broad-band measurement in W m^{-2}) of a hypothetical UV-B meter. The response of this meter at environmentally relevant wavelengths (>295 nm) approximates the SWF for sunburn, but some might consider the readings to represent UV-B. The relatively inexpensive meter would report total UV-B irradiance (i.e., W m^{-2} , 290 - 320 nm) accurately for midday clear-sky solar irradiance at 45° latitude at the equinox. The 1:1 relationship between this measure and unweighted UV-B irradiance would vary for other locations, times, depths, and sources of irradiance (see Table 1).

Such an instrument can be calibrated to report UV-B (W m^{-2}) accurately for a particular source of irradiance (Table 1, cell 1B), but because instrument response is not directly proportional to energy for wavelengths between 280 and 320 nm, the proportionality between the meter reading and UV-B irradiance will change with spectral shape of the source. For example, our hypothetical UV-B meter would overestimate the increase of UV-B with ozone depletion (B4 vs B3, B8 vs B7) because it weights the shorter wavelengths heavily (Fig. 2D). The discrepancy between UV-B and that measured by the meter is much greater for comparisons of laboratory exposures with the solar irradiance at mid-latitude (H9 vs I9, H10 vs I10). Thus, when a laboratory experiment is compared to a natural exposure on the basis of broad-band UV-B measurements, the comparison should be considered approximate at best, unless it can be shown that the spectral sensitivity of the biological process closely matches the spectral response of the UV-B sensor. We have not explored in detail the use of broad-band sensors to measure the penetration of UV-B in natural waters (column 6). Kirk et al.³² show clearly that such sensors are unsatisfactory for underwater use because they cannot distinguish between light fields that may have the same measured UV-B, but different spectral distributions, hence different biological effects. Some sensors match the response for erythema³⁴ so their general use is appropriate if one wishes to quantify the potential for sunburn, or a process with a closely similar SWF.

The conditions represented in Table 1 are arbitrarily chosen, so it is not possible to generalize broadly about how well a broad-band sensor might represent biologically effective irradiance for processes such as damage to DNA and inhibition of photosynthesis. Clearly, errors are introduced, and they are worse for SWFs that differ greatly from the response function of the meter.

Different weighting functions to describe similar processes. Weighting functions are available to quantify biologically effective irradiance for several processes,¹⁹ but their generality is not guaranteed. For example, Setlow's¹⁶ generalized DNA damage function is consistent with the action spectrum for DNA damage in phages, but for alfalfa seedlings it overestimates the effect of wavelengths <310 nm, presumably because of absorption in the seedlings by cellular material other than DNA.¹⁵ Organisms with other geometries and with UV-absorbing compounds³⁵ would be expected to have different action spectra for damage to DNA. Likewise, BWFs for inhibition of photosynthesis vary in shape (i.e., the slope of $\frac{I}{I_0}$ vs wavelength) and in absolute sensitivity.¹³ Note that relative BWFs normalized to 1.0 at a particular wavelength (Fig. 1, refs. 21,23,24) can describe differences in shape between spectra, but not differences in biological effect for a given wavelength.

An important implication of differences between SWFs has been well described in the literature: lower weightings for UV-B (which is influenced by ozone depletion) as compared to UV-A (which is not) reduce predicted impacts of ozone depletion.^{15,19} This pattern is reflected in Table 1, where the steep Setlow action spectrum for DNA predicts the greatest increases of effect with ozone depletion (Table 1; C4 vs C3 and C8 vs C7). Comparisons between two similarly-determined BWFs for inhibition of photosynthesis (*Phaeodactylum* grown in the laboratory, and Antarctic phytoplankton in outdoor culture; see Fig. 1) show that the predicted effects of ozone depletion would be somewhat higher using the laboratory result (relative increases for ozone hole vs normal ozone; rows M vs N). As for other SWFs, the biggest differences between the two photoinhibition BWFs are associated with the comparisons between natural irradiance and laboratory exposures to sunlamps.

How should radiant exposure during experiments be described if the BWF is unknown? Presentation of the experimental irradiance spectrum in absolute units is always useful. Further, we recommend that irradiance be weighted by several published SWFs and that each weighted exposure should be reported. Later, it may be known which spectrum is best for the process being studied.

Temporal Dependence and Reciprocity of UV Effects

We have shown that it is critical to use the correct BWF for describing biologically effective irradiance, but we have not yet discussed how BWFs are determined. It is necessary to consider another issue first: how the time-dependence of UV effects may influence the relationship between

radiant exposure and the measured response, i.e., the exposure response curve (ERC³⁶). This subject has been addressed directly,^{6,7,18,28,36-39} and will be treated only briefly here.

For a process that is essentially irreversible over the time-scale considered, the measured effect should be a function solely of cumulative exposure (weighted with the appropriate SWF): that is, reciprocity should hold. Reciprocity is satisfied when the effect of a total radiation exposure is independent of the time over which the exposure occurs, i.e., cumulative effect is the same, regardless of exposure rate.^{18,28} Reciprocity is assumed when measurements made over different periods of time are plotted together and described analytically as a function of cumulative exposure (biologically effective J m⁻² or equivalent). When reciprocity fails, plots of effect vs cumulative exposure lose meaning,²⁸ and attempts to determine wavelength-dependence are compromised. The assumption of reciprocity, either explicit or implicit, is common to many studies of UV effects,^{18,21,30,40,41} but dependence on irradiance has also been explicitly assumed (refs. 42,43, based on refs. 14 and 22 respectively). The assumption can be tested rigorously with controlled exposures at widely different fluence rates over a range of time periods,^{28,44} but it has been evaluated only partially in the field,^{21,29} where experimental exposures to modified solar irradiance are difficult to control and quantify (see discussion in ref. 6).

Reciprocity for the inhibition of photosynthesis by UV-B radiation has been tested in the laboratory.²⁸ Cultures of a marine diatom growing at 20°C were exposed to different irradiances of supplementary UV-B for periods of 4 h. The rate of photosynthesis declined in response to UV-B, and within about 30 min reached a rate that was maintained for the remainder of the experiment. The inhibited rate could be described as a hyperbolic function of UV-B irradiance, consistent with a dynamic balance between damage and repair.³⁷ The shape of the hyperbolic function (i.e., P , relative to the uninhibited control = $1/[1 + E^*]$) was insensitive to biological weighting, because supplemental UV-B was varied with neutral density screens so that any weighted irradiance would be equivalent when normalized to full exposure. Because the inhibited rate of photosynthesis depended on exposure rate, it could not be described solely as a function of cumulative exposure. This failure of reciprocity supported the assumption that the inhibition of photosynthesis by UV could be described as a function of biologically weighted irradiance (i.e., the BWF-PI model, with weightings, $[W]$, having units of reciprocal W m⁻²).¹⁴

Subsequently, we observed a contrasting response: for phytoplankton from open waters of the Antarctic at 0°C, reciprocity was well satisfied for the inhibition of photosynthesis by UV.^{27,45} Rates of damage were similar to what was studied in the laboratory, so the difference in kinetic response might be due to sluggish repair associated with lower temperature, and perhaps low growth rates of

the deeply-mixed Antarctic phytoplankton. Regardless of the mechanistic basis, this fundamentally different response demanded a fundamentally different model for describing the relationship between UV exposure and effect. Consequently, the BWF_H -PI model was developed (H is the symbol for cumulative exposure in $J\ m^{-2}$), in which the cumulative effect of inhibition is described as the integral of a semi-logarithmic survival curve.⁴⁶ In this model, biological weightings, $\varpi_H(\lambda)$, have units of reciprocal $J\ m^{-2}$ and are applied to measurements of cumulative exposure.²⁷

Because reciprocity can hold under some conditions, and not under others, the assumption of reciprocity must be considered explicitly when relating biological effect to radiant exposure. That is, results must be expressed as functions of irradiance or cumulative exposure, and the choice should be justified — preferably by explicit rejection of the alternate model. If all experimental exposures are to unvarying irradiance treatments for the same duration, however, the question can be deferred: in a relative sense, irradiance is exactly equivalent to cumulative exposure, and wavelength-dependent biological effectiveness can be determined, if only for that time-scale. To extrapolate to other time scales, one must understand, specify and parameterize the time-dependence.

Linearity of the Exposure vs Response Curve

If the reciprocity issue is resolved, and biologically effective irradiance (or cumulative exposure) is weighted with an appropriate BWF, then a biological effect can be related to radiant exposure in a quantitative, generalizable function. Indeed, one way of testing a BWF is to see how well it reduces scatter in the relationship between effect and weighted exposure.¹⁸ In turn, a BWF can be determined statistically by finding the weightings that minimize unexplained variability in the exposure response curve (ERC).^{1,14}

The fundamental model that relates effect to weighted exposure is no less important than a BWF for quantifying and generalizing the influence of UV on biological processes. That is, to quantify how well a BWF minimizes scatter in the relationship between response and exposure, one must specify the shape (i.e., functional form) of the ERC.³⁶ Consider the induction of dimer formation in DNA by UV-B: death ensues when only a small fraction of the DNA has been damaged,⁴⁷ long before the rate of damage would decline due to a significant reduction in susceptible base pairs. Consequently, cumulative damage can be accurately described as a linear function of cumulative exposure.¹⁵ Processes that repair DNA³⁵ will influence the relationship between net damage and cumulative exposure.

Inhibition of photosynthesis is a different story. Commonly, rates of photosynthesis much less than 50% of a PAR-only control are measured for samples incubated several hours at surface

irradiance (e.g., refs. 29,41,48). Linearity of cumulative effect (inhibition of photosynthesis relative to PAR-only control) vs cumulative exposure (weighted by a BWF or reported as some measure proportional to biologically weighted exposure) is neither expected nor generally observed. Why? 1) if the response is consistent with laboratory results (Fig. 4A),^{28,37} reciprocity would fail and inhibition will be a hyperbolic function of weighted irradiance (dimensionless E^* or $W m^{-2}_{\text{Beff}}$); and 2) if the process is essentially irreversible over the time-scale of damage and inhibition is a function of effective irradiance times the absorption cross section of undamaged photosynthetic systems, photosynthetic rate will decrease as a nearly linear function of cumulative exposure (dimensionless H^* or $J m^{-2}_{\text{Beff}}$), only as long as the number of susceptible targets in the photosynthetic apparatus has not significantly decreased. As the latter condition occurs (it would certainly be the case when cumulative photosynthesis is less than 50% relative to a control), the decrease in photosynthesis would become noticeably nonlinear (Fig. 4B), consistent with a semi-logarithmic survival curve (see ref. 46). It would be instructive to consider these two types of underlying models when relating complex biological processes to radiant exposure, remembering that the shape of the ERC can be distorted if an inappropriate BWF is applied.

Nonlinearity in the relationship between exposure and response should be considered explicitly

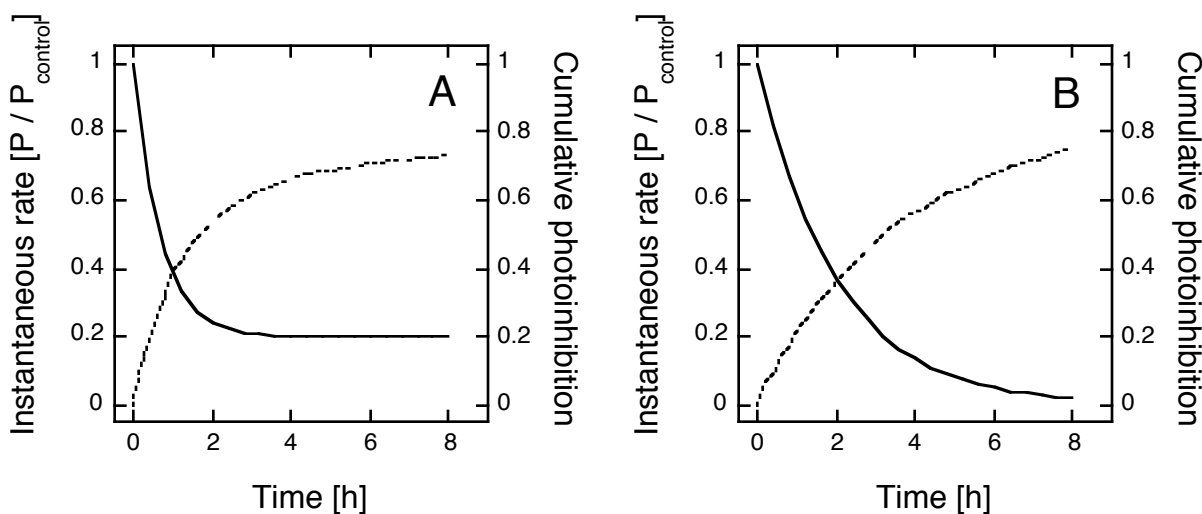


Fig. 4: Kinetics of photosynthesis during photoinhibition according to different models, adjusted to describe similar degrees of inhibition for cumulative photosynthesis over about 8 h: each plot shows instantaneous photosynthesis, relative to an uninhibited control (P/P_{control} ; solid line), and cumulative photoinhibition, expressed as $1 - \text{cumulative photosynthesis relative to the control}$ (dotted line). A) P/P_{control} declines to a dynamic balance between damage and repair;³⁷ and B) P/P_{control} is reduced consistent with a survival curve (see text). Constant irradiance is assumed: thus, time is directly proportional to cumulative exposure.

when estimating the potential influences of ozone depletion. Given an appropriate spectral weighing function and calculations of solar spectral irradiance as a function of column ozone, it is possible to estimate a radiation amplification factor (RAF), a coefficient that quantifies the nonlinear change in effective irradiance as a function of the change in column ozone:^{7,19,49}

$$\frac{E_1^*}{E_2^*} = \left(\frac{\square_1}{\square_2} \right)^{\square_{RAF}} \quad (2)$$

where E_1^* and E_2^* represent biologically effective irradiance at column ozone amounts \square_1 and \square_2 , respectively. If the biological effect is a nonlinear function of E^* , then the ratios of effective irradiance predicted by an RAF will not directly reflect the influence of ozone depletion. In such cases, the relationship between biological effect and column ozone should be described with a total amplification factor that incorporates the nonlinear relationship between E^* and biological effect.⁷

To reiterate: whether one is estimating a BWF given observations of UV-dependent responses, or predicting the influences of altered UV by using a spectral weighting function, it is crucial that biological effect is appropriately related to radiant exposure with an ERC. That is, the time-dependence and linearity of the exposure-response relationship must be known or assumed.

Methods for Determining Biological Weighting Functions

The features necessary for determining environmentally relevant BWFs have been reviewed.⁵ It is strongly emphasized that the irradiance treatments should consist of progressively greater amounts of first UV-A, then UV-B, added to a constant background of visible (PAR) irradiance.² This polychromatic approach for BWFs contrasts with the monochromatic approach appropriate for action spectra, which involves measuring the effects of illumination with only a narrow band of radiation, thereby reducing or eliminating counteracting processes that may be stimulated by other wavelengths.^{47,50,51} The monochromatic approach can be useful for determining the nature of damage, but it is not satisfactory for representing the net effect in nature.

Rundel¹ tackled the challenge of estimating BWFs from data on photosynthetic responses to polychromatic exposures. In general, the data show an increasingly greater effect (e.g. more severe inhibition of photosynthesis) associated with successively higher ratios of UV:PAR as shorter wavebands of UV were transmitted to the treatment. A simple analysis is to order the results by irradiance of UV exposure (W m^{-2}) and to compute the difference in inhibition between successive treatments. Then the biological weight for each waveband is estimated as the differential effect divided by the difference in energy between the treatments that include and exclude that waveband.

However, as Rundel pointed out, the estimated weight may be inaccurate if the actual response changes rapidly over the wavelengths for which the treatments differ (the differential bandwidth is usually on the order of 15-20 nm). Moreover, there is no objective method to determine the central wavelength for a weighting. Initial estimates of the biological weighting function for inhibition of photosynthesis by Antarctic phytoplankton were based on this approach,^{24,52} and results were used to calculate the relative increase of biologically damaging irradiance associated with Antarctic ozone depletion.

As an alternative to the simple differential method, Rundel advocated assuming *a priori* that the BWF is a general function, e.g., that the natural log of the BWF is a polynomial:

$$\ln(W) = e^{(a_0 + a_1\lambda + a_2\lambda^2 + \dots)} \quad (3)$$

Many BWFs can be approximated by such a general exponential function (Fig. 1; see also refs. 21 and 22). In practice, the parameters for the BWF polynomial (a_i) are estimated by non-linear regression (see ref. 53 and Appendix 1). The general function can be modified to introduce various complexities (e.g. thresholds), but the increased complexity should be justified statistically. For example, the fit should initially be performed for a first order exponential function (a_0 and a_1); higher order functions can be tested, but they should be accepted only if they significantly increase the amount of experimental variance explained. The standard errors of the parameter estimates from the non-linear regression are used to calculate the uncertainty in estimates of $\ln(W)$.⁵⁴

Many published SWFs decrease monotonically to zero with increasing wavelength. However, most of these spectra have been determined for “simple” processes (e.g. DNA dimerization) using monochromatic treatments. On the other hand, processes in living organisms are usually the net result of competing photo-dependent mechanisms that are all active during polychromatic treatment.^{30,48,55} In particular, this means that weights may at times be negative (beneficial effects outweigh damage, e.g. ref. 13; see also refs. 22,48) and may not decrease monotonically to zero with increasing wavelength, as equation 3 specifies. Choosing a model and justifying it statistically can be difficult under such circumstances, unless one has a large number of treatments or very precise results.

We have developed an alternative method of fitting high resolution BWFs which does not require *a priori* choice of the shape of the weighting function. In this technique (refs. 13,14 and Appendix 1), UV spectral irradiance in each treatment is analyzed by Principal Component Analysis (PCA) to generate up to four principal components (essentially, statistically independent shapes

defined by weights for each wavelength) which account for nearly 100% of the variance of the treatment spectra relative to the mean spectrum. Component scores (the relative contribution, c_i , of each principal component, i , to a given UV spectrum, normalized to PAR) are derived for each of the treatment spectra. The estimation of the BWF then proceeds by non-linear regression as for the Rundel method, except that the parameters estimate the importance of each spectral component to the measured response, i.e. we estimate coefficients m_i such that $E^* = E_{\text{PAR}}(m_0 + \sum_{i=1}^4 m_i c_i)$, where E_{PAR} is PAR in W m^{-2} , m_0 is the coefficient for the contribution to photoinhibition of PAR plus the mean spectrum, and m_i are the contributions of the spectral components. Again, only as many components are incorporated into the final estimate as can be justified based on variance explained. Finally, once the m_i are estimated by regression, the $\square\square$ estimates and their respective statistical uncertainty can be calculated via the original spectral components. Details of the method are given in refs. 13,14, and Appendix 1. Pertinent observations are that the calculated BWFs generally explain > 90% of the variance in photosynthesis of 72 samples, and that the weighting functions can and do show features more complex than simple exponential slopes.

Accepting that the polychromatic approach is required to determine BWFs for many biological processes, and judging by publications to date, it seems that the Rundel method and the PCA method are the procedures of choice for the statistical estimation of BWFs in aquatic systems. How do they compare? As a guide to the application of the Rundel and PCA methods, we offer a couple of concrete examples. Data for calculation of several BWFs for UV inhibition of photosynthesis in Antarctic phytoplankton were acquired during a cruise to the Weddell-Scotia Confluence (WSC), during the Austral Spring of 1993. Details of sample collection, experimental procedures and primary photosynthetic data are described in ref. 27. Here we focus on the results from two stations where BWFs were estimated from duplicated sets of 72 measurements of photosynthesis under different spectral irradiance treatments for incubations of 1 h. The BWFs were estimated for the $\text{BWF}_H/\text{P-I}$ model (consistent with the kinetics of Fig. 4B) using both the Rundel and PCA method. No significant increase in variance explained (R^2) was obtained by using a polynomial with more than linear terms in the exponent for the Rundel method (eq. 3), or by including more than 2 principal components in the PCA method. We did not attempt to introduce thresholds. The PCA-fit BWFs are consistent with the overall slope of the Rundel estimated BWFs, with the PCA BWFs within the estimated 95% confidence interval for the Rundel BWFs over the 290-400 nm region most relevant to solar exposure (Fig. 5). Both fits are consistent with a 3-4 times greater \square_H (higher sensitivity to UV inhibition) for phytoplankton from a station with a deeply mixed surface layer (Station P') as compared to a station with a more shallow mixed layer (Station P).²⁷ Overall, both methods resulted in a similar total variance explained ($R^2 = 0.90-0.94$). Thus, either method is

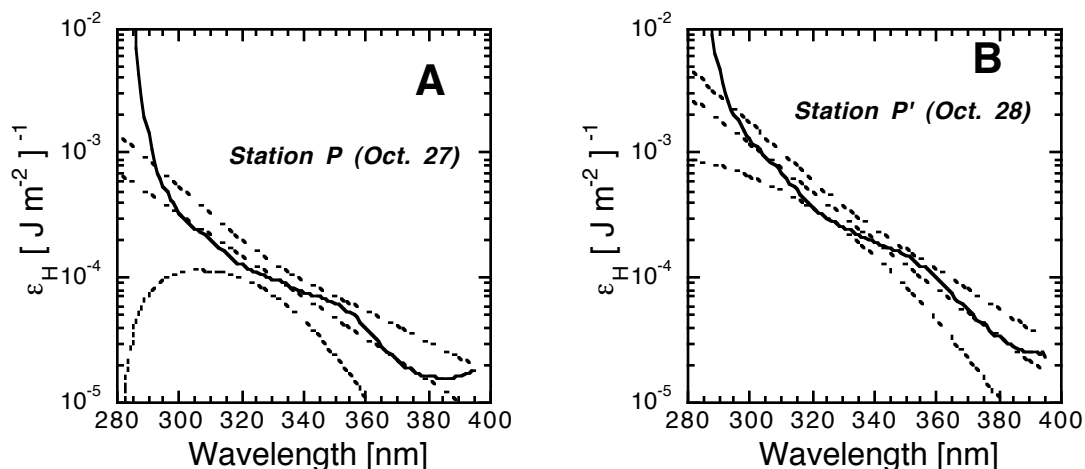


Figure 5. Biological weighting functions for inhibition of photosynthesis, dependent on cumulative exposure (\square_h , $[\text{J m}^{-2}]^{-1}$; for exposures of 1 h, consistent with the kinetic model in Fig. 4B), based on photoinhibitor measurements¹⁴ in the Weddell-Scotia Confluence (WSC, Southern Ocean) during austral spring 1993. Statistical fits were made using the Rundel method (dotted lines, $\pm 95\%$ confidence intervals) and the PCA method (solid lines) for phytoplankton samples near the surface at two stations in the WSC: A) Station P, with a relatively UV-tolerant assemblage; and B) Station P', where a relatively UV-sensitive assemblage was sampled. Full experimental details are given in ref. 27. Calculations are outlined in the Appendix.

appropriate to fitting BWFs based on the measurements in polychromatic incubations using a large number of spectral treatments. However, the PCA method can capture possible peaks or valleys in the BWF which are not resolved by the general polynomial function. Preliminary results with estuarine dinoflagellates suggest that such features can occur when cells contain high amounts of UV-absorbing compounds (Neale et al.; unpubl.). The PCA method is more versatile in that it should automatically adjust to any changes in the true shape of spectral response function. For example, the BWF at another WSC station had $\square_h < 0$ for the near UV-A range ($\lambda > 360$ nm). This could be estimated using the Rundel method by adding an arithmetic offset to equation 3.

Summary and Conclusions

Relying on examples, real and idealized, rather than on a comprehensive review of the literature, we have illustrated some key considerations for describing the influence of ultraviolet radiation on aquatic systems. Several points bear repeating.

- 1) If an effect of UV is expressed as a function of radiant exposure for regimes with different spectral irradiance (i.e., different depths in the water column, times of day or year, or different artificial sources of UV), a weighting function is used, either explicitly or implicitly.

- 2) The quantitative comparison of different radiant exposures can be very sensitive to the weighting function that is chosen: if the wrong weighting function is used and spectral shape differs strongly between treatments, comparisons can be grossly inaccurate.
- 3) Broad-band meters are in many cases unsatisfactory for comparing biologically effective exposures, and they are inappropriate for describing the penetration of biologically effective irradiance in surface waters.
- 4) To characterize the influence of UV on a biological process, one should determine the degree to which effect is a function of cumulative exposure, independent of exposure rate (or vice-versa), and analyze experimental results accordingly.
- 5) For some biological processes, such as the inhibition of photosynthesis, the relationship between effect and radiant exposure is unlikely to be linear. If nonlinearity is a feature of biological response, it should be incorporated into descriptive as well as predictive models, and radiation amplification factors should be adjusted to calculate total amplification factors.
- 6) Polychromatic exposures (PAR, with increments of increasingly shorter wavelengths of UV) should be used to determine environmentally relevant biological weighting functions. Results can be obtained with an exponential curve-fitting method¹ or through the use of multivariate analysis and curve fitting.^{14,27} Both methods can reveal the principal features of BWFs, but the multivariate method can discern more detail.

This discussion is no substitute for the dozens of publications in which the underlying principles have been developed — new experiments and better radiometers will help us to describe better the effects of UV on aquatic systems, but the library remains one of our most valuable research tools.

Acknowledgments

Support from NSERC Canada, NASA, and NSF Polar Programs is gratefully acknowledged. Suggestions from D.-P. Häder and an anonymous reviewer are appreciated. CEOTR publication xxx.

References

1. Rundel RD. Action spectra and estimation of biologically effective UV radiation. *Physiol Plant* 1983; 58:360-366.
2. Caldwell MM, Camp LB, Warner CW, et al. Action spectra and their key role in assessing biological consequences of solar UV-B radiation change. In: Worrest RC, Caldwell MM, eds. *Stratospheric Ozone Reduction, Solar Ultraviolet Radiation and Plant Life*. New York: Springer, 1986:87-111.
3. Coohill TP. Ultraviolet action spectra (280 to 380 nm) and solar effectiveness spectra for higher plants. *Photochem Photobiol* 1989; 50:451-457.
4. Smith RC, Baker KS. Stratospheric ozone, middle ultraviolet radiation and phytoplankton productivity. *Oceanogr Mag* 1989; 2(2):4-10.
5. Coohill TP. Action spectra again? *Photochem Photobiol* 1991; 54:859-870.
6. Cullen JJ, Neale PJ. Ultraviolet radiation, ozone depletion, and marine photosynthesis. *Photosyn Res* 1994; 39:303-320.
7. Smith RC, Cullen JJ. Effects of UV radiation on phytoplankton. *Rev Geophys* 1995; Suppl., U.S. National Report to the IUGG 1991-1994:1211-1223.
8. Kirk JTO. *Light and Photosynthesis in Aquatic Ecosystems*. (2nd ed.) Cambridge: Cambridge University Press, 1994.
9. Morel A. Available, usable, and stored radiant energy in relation to marine photosynthesis. *Deep-Sea Res* 1978; 25:673-688.
10. Harrison WG, Platt T, Lewis MR. The utility of light-saturation models for estimating marine primary productivity in the field: a comparison with conventional "simulated" in situ methods. *Can J Fish Aquat Sci* 1985; 42:864-872.
11. Sakshaug E, Johnsen G, Andersen K, et al. Modeling of light-dependent algal photosynthesis and growth: experiments with Barents Sea diatoms *Thalassiosira nordenskiöldii* and *Chaetoceros furcellatus*. *Deep-Sea Res* 1991; 38:415-430.
12. Jones LW, Kok B. Photoinhibition of chloroplast reactions. I. Kinetics and action spectra. *Plant Physiol* 1966; 41:1037-1043.
13. Neale PJ, Lesser MP, Cullen JJ. Effects of ultraviolet radiation on the photosynthesis of phytoplankton in the vicinity of McMurdo Station, Antarctica. In: Weiler CS, Penhale PA, eds. *Ultraviolet Radiation in Antarctica: Measurements and Biological Effects*. Washington, D.C.: American Geophysical Union, 1994:125-142. Antarctic Research Series; vol 62.
14. Cullen JJ, Neale PJ, Lesser MP. Biological weighting function for the inhibition of phytoplankton photosynthesis by ultraviolet radiation. *Science* 1992; 258:646-650.

15. Quate FE, Sutherland BM, Sutherland JC. Action spectrum for DNA damage in alfalfa lowers predicted impact of ozone depletion. *Nature* 1992; 358:576-578.
16. Setlow RB. The wavelengths in sunlight effective in producing skin cancer: a theoretical analysis. *Proc Natl Acad Sci USA* 1974; 71(9):3363-3366.
17. Smith RC. Ozone, middle ultraviolet radiation and the aquatic environment. *Photochem Photobiol* 1989; 50(4):459-468.
18. Smith RC, Baker KS, Holm-Hansen O, et al. Photoinhibition of photosynthesis in natural waters. *Photochem Photobiol* 1980; 31:585-592.
19. Madronich S. Increases in biologically damaging UV-B radiation due to stratospheric ozone reductions: A brief review. *Arch Hydrobiol Beih Ergebn Limnol* 1994; 43:17-30.
20. Häder D-P, Worrest RC. Effects of enhanced solar ultraviolet radiation on aquatic ecosystems. *Photochem Photobiol* 1991; 53(5):717-725.
21. Behrenfeld MJ, Chapman JW, Hardy JT, et al. Is there a common response to ultraviolet-b radiation by marine phytoplankton. *Mar Ecol Prog Ser* 1993; 102:59-68.
22. Boucher N, Prézelin BB. An *in situ* biological weighting function for UV inhibition of phytoplankton carbon fixation in the Southern Ocean. *Mar Ecol Prog Ser* 1996; :in press.
23. Helbling EW, Villafañe V, Ferrario M, et al. Impact of natural ultraviolet radiation on rates of photosynthesis and on specific marine phytoplankton species. *Mar Ecol Prog Ser* 1992; 80:89-100.
24. Lubin D, Mitchell BG, Frederick JE, et al. A contribution toward understanding the biospherical significance of Antarctic ozone depletion. *J Geophys Res* 1992; 97(D8):7817-7828.
25. Booth CR, Lucas TB, Morrow JH, et al. The United States National Science Foundation's polar network for monitoring ultraviolet radiation. In: Weiler CS, Penhale PA, eds. *Ultraviolet Radiation in Antarctica: Measurements and Biological Effects*. Washington, D.C.: American Geophysical Union, 1994:17-37. Antarctic Research Series; vol 62.
26. Gregg WW, Carder KL. A simple spectral solar irradiance model for cloudless maritime atmospheres. *Limnol Oceanogr* 1990; 35(8):1657-1675.
27. Neale PJ, Cullen JJ, Davis RF. Inhibition of marine photosynthesis by ultraviolet radiation: Variable sensitivity of phytoplankton in the Weddell-Scotia Sea during austral spring. *Limnol Oceanogr* 1996; in prep
28. Cullen JJ, Lesser MP. Inhibition of photosynthesis by ultraviolet radiation as a function of dose and dosage rate: Results for a marine diatom. *Mar Biol* 1991; 111:183-190.
29. Helbling EW, Villafañe V, Holm-Hansen O. Effects of ultraviolet radiation on Antarctic marine phytoplankton photosynthesis with particular attention to the influence of mixing. In: Weiler CS, Penhale PA, eds. *Ultraviolet Radiation in Antarctica: Measurements and*

- Biological Effects. Washington, D.C.: American Geophysical Union, 1994:207-227. Antarctic Research Series; vol 62.
30. Smith RC, Prézelin BB, Baker KS, et al. Ozone depletion: Ultraviolet radiation and phytoplankton biology in Antarctic waters. *Science* 1992; 255:952-959.
 31. Green AES, Cross KR, Smith LA. Improved analytic characterization of ultraviolet skylight. *Photochem Photobiol* 1980; 31:59-65.
 32. Kirk JTO, Hargreaves BR, Morris DP, et al. Measurement of UV-B in two freshwater lakes: an instrument intercomparison. *Arch Hydrobiol Beih Ergebn Limnol* 1994; 43:71-99.
 33. Smith RC, Wan Z, Baker KS. Ozone depletion in Antarctica - Modeling its effect on solar UV irradiance under clear-sky conditions. *J Geophys Res* 1992; 97:7383-7397.
 34. Smith GJ, White MG, Ryan KG. Seasonal trends in erythemal and carcinogenic ultraviolet radiation at mid-southern latitudes 1989-1991. *Photochem Photobiol* 1993; 57(3):513-517.
 35. Karentz D. Ultraviolet tolerance mechanisms in Antarctic marine organisms. In: Weiler CS, Penhale PA, eds. *Ultraviolet Radiation in Antarctica: Measurements and Biological Effects*. Washington, D.C.: American Geophysical Union, 1994:93-110. Antarctic Research Series; vol 62.
 36. Coohill TP. Exposure response curves action spectra and amplification factors. In: Biggs RH, Joyner MEB, eds. *Stratospheric Ozone Depletion / UV-B Radiation in the Biosphere*. Berlin: Springer, 1994:57-62. NATO ASI Series; vol 118.
 37. Lesser MP, Cullen JJ, Neale PJ. Carbon uptake in a marine diatom during acute exposure to ultraviolet B radiation: Relative importance of damage and repair. *J Phycol* 1994; 30:183-192.
 38. Vincent WF, Roy S. Solar ultraviolet-B radiation and aquatic primary production: damage, protection and recovery. *Environ Rev* 1993; 1:1-12.
 39. Smith RC, Baker KS. Assessment of the influence of enhanced UV-B on marine primary productivity. In: Calkins J, ed. *The Role of Solar Ultraviolet Radiation in Marine Ecosystems*. New York: Plenum Press, 1982:509-537.
 40. Behrenfeld M, Hardy J, Gucinski H, et al. Effects of ultraviolet-B radiation on primary production along latitudinal transects in the south Pacific Ocean. *Mar Environ Res* 1993; 35:349-363.
 41. Vernet M, Brody EA, Holm-Hansen O, et al. The response of Antarctic phytoplankton to ultraviolet radiation: absorption, photosynthesis, and taxonomic composition. In: Weiler CS, Penhale PA, eds. *Ultraviolet Radiation in Antarctica: Measurements and Biological Effects*. Washington, D.C.: American Geophysical Union, 1994:143-158. Antarctic Research Series; vol 62.
 42. Arrigo KR. Impact of ozone depletion on phytoplankton growth in the Southern Ocean: large-scale spatial and temporal variability. *Mar Ecol Prog Ser* 1994; 114:1-12.

43. Boucher NP, Prézelin BB. Spectral modeling of UV inhibition of *in situ* Antarctic primary production using a field derived biological weighting function. *Photochem Photobiol* 1996; :in press.
44. Blakefield MK, Calkins J. Inhibition of phototaxis in *Volvox aureus* by natural and simulated solar ultraviolet light. *Photochem Photobiol* 1992; 55:867-872.
45. Cullen JJ, Neale PJ, Davis RF, et al. Ultraviolet radiation, vertical mixing, and primary productivity in the Antarctic. *EOS* 1994; 75(3):200.
46. Harm HW. Biological effects of ultraviolet radiation. 1980. I.U.P.A.B. Biophysics;
47. Karentz D, Cleaver JE, Mitchell DL. Cell survival characteristics and molecular responses of Antarctic phytoplankton to ultraviolet-B radiation. *J Phycol* 1991; 27:326-341.
48. Prézelin BB, Boucher NP, Smith RC. Marine primary production under the influence of the Antarctic ozone hole: Icecolors '90. In: Weiler CS, Penhale PA, eds. *Ultraviolet Radiation in Antarctica: Measurements and Biological Effects*. Washington, D.C.: American Geophysical Union, 1994:159-186. Antarctic Research Series; vol 62.
49. Booth CR, Madronich S. Radiation amplification factors: Improved formulation accounts for large increases in ultraviolet radiation associated with Antarctic ozone depletion. In: Weiler CS, Penhale PA, eds. *Ultraviolet Radiation in Antarctica: Measurements and Biological Effects*. Washington, D.C.: American Geophysical Union, 1994:39-42. Antarctic Research Series; vol 62.
50. Hirosawa T, Miyachi S. Inactivation of Hill reaction by long-wavelength radiation (UV-A) and its photoreactivation by visible light in the cyanobacterium, *Anacystis nidulans*. *Arch Microbiol* 1983; 135:98-102.
51. Samuelsson G, Lönneborg A, Rosenqvist E, et al. Photoinhibition and reactivation of photosynthesis in the cyanobacterium *Anacystis nidulans*. *Plant Physiol* 1985; 79:992-995.
52. Mitchell BG. Action spectra of ultraviolet photoinhibition of Antarctic phytoplankton and a model of spectral diffuse attenuation coefficients. In: Mitchell BG, Holm-Hansen O, Sobolev I, eds. *Response of Marine Phytoplankton to Natural Variations in UV-B Flux*. Washington, D.C.: Chemical Manufacturers Association, 1990:Appendix H.
53. Marquardt DW. An algorithm for least-squares estimation of nonlinear parameters. *J Soc Ind Appl Math* 1963; 11:431-441.
54. Bevington PR. *Data Reduction and Error Analysis for the Physical Sciences*. New York: McGraw Hill, 1969.
55. Quesada A, Mouget J-L, Vincent WF. Growth of Antarctic cyanobacteria under ultraviolet radiation: UVA counteracts UVB inhibition. *J Phycol* 1995; 31:242-248.

Appendix 1: Procedures for Calculating Biological Weighting Functions

Here we describe how to calculate BWFs, using both the exponential weighting method¹ and the PCA method.^{2,3} The inhibition of photosynthesis is used as an example, but the principles are essentially the same for calculating any BWF. The procedure is to quantify photosynthesis under different well-measured spectral treatments, using long-pass optical filters to include progressively shorter wavelengths of UV along with PAR; the reduction of photosynthesis associated with inclusion of shorter wavelengths is described quantitatively with spectral weighting coefficients, $w(\lambda)$. It is common to use one PAR-only treatment as a control, and about 4 - 6 treatments with different cut-off wavelengths for UV. Here, we describe a more general analysis: photosynthesis is measured as the uptake of ¹⁴C-bicarbonate during controlled exposures to temporally constant irradiance in each of 72 spectral treatments: the ratios of UV:PAR are varied with long-pass filters (8 spectral treatments), and within each spectral treatment, neutral density screens are used to generate nine treatments with similar UV:PAR, but with a broad range of PAR irradiance.² Whether one or many PAR irradiance exposures are used, the objective is to describe the UV-dependent reduction of photosynthetic rate.

1: Start with an underlying model. A functional relationship between exposure and response (i.e., an algebraic representation of the exposure response curve) must first be chosen and justified. In its most general form, the inhibition of photosynthesis as a function of biologically effective irradiance (E^* , dimensionless) and time (t) is:

$$\left(\frac{P}{P_{\text{pot}}}\right)_t = f(E^*, t) \quad (\text{A1})$$

where P_{pot} (“pot” for potential) is the uninhibited rate of photosynthesis, dependent on PAR, and P is the instantaneous rate of photosynthesis ($\text{mg C m}^{-3} \text{ h}^{-1}$) measured under a combination of PAR and UV. For the following examples, we use a model appropriate for the inhibition of photosynthesis in natural phytoplankton from open waters of the Antarctic, where reciprocity was verified for time scales from about 0.5 to 2 h (see ref. 5). The model (Fig. 4B) is

$$\left(\frac{P}{P_{\text{pot}}}\right)_t = e^{-H^*} \quad (\text{A2})$$

where H^* at any time t is biologically weighted irradiance (Eq. 1) integrated through time:

$$H^* = \int_0^t \left(\int_{\lambda=280\text{nm}}^{400\text{nm}} w_H(\lambda) \cdot E(\lambda) \cdot w(\lambda) d\lambda \right) dt \quad (\text{A3})$$

The weightings $[w_H(I)]$, reciprocal J m^{-2} define the BWF for inhibition of photosynthesis. The subscript (H , for radiant exposure, J m^{-2}) distinguishes this dose-dependent weighting from the irradiance-dependent weighting in equation 1.

Because this model is time-dependent, we must account for cumulative photosynthesis over the duration of the experiment (time = 0 to T) by integrating equation A2,

$$\int_0^T \frac{P_t}{P_{\text{pot}}} dt = \frac{(1 - e^{-H_t^*})}{H_t^*} \cdot T \quad (\text{A4}).$$

Cumulative photosynthesis is then expressed as an average rate over the incubation period, T :

$$\frac{P_{\text{avg}}}{P_{\text{pot}}} = \frac{(1 - e^{-H^*})}{H^*} \quad (\text{A5}).$$

This is the exposure response curve (ERC). For our experiments, P_{pot} is independent of time because irradiance is constant within treatments.

Given the ERC, our task is to calculate biological weightings for H^* (Eq. A3) comparable to those for E^* in equation 1 of the main text. The weightings $[w_H(I)]$ that determine H are incorporated into a model of photosynthesis as a function PAR, as influenced by biologically weighted UV:

$$P_{\text{avg}} = \underbrace{P_s (1 - e^{-E_{\text{PAR}}/E_k})}_{P_{\text{pot}}} \cdot \underbrace{\frac{(1 - e^{-H^*})}{H^*}}_{P_{\text{avg}}/P_{\text{pot}}} \quad (\text{A6}).$$

Uninhibited photosynthesis (P_{pot}) is a saturation function of E_{PAR} , defined by the maximal rate of photosynthesis (P_s) and a saturation irradiance (E_k).⁶ Nonlinear curve-fitting is used to minimize unexplained error in equation (A6), generating estimates of P_s , E_k , and the BWF coefficients, $[w_H(I)]$. We generally normalize photosynthesis to initial chlorophyll concentration, thereby yielding estimates of P^B ($\text{mg C mg Chl}^{-1} \text{ h}^{-1}$) that are used commonly in models of productivity; the BWF is unaffected by such normalization, and the superscript will be omitted here.

Table A1. Symbols and abbreviations. Ranges refer to an experiment with 72 spectral treatments and measurements of spectral irradiance at 121 wavelengths from 280 nm to 400 nm.

Symbol	Meaning	Units
a_0	first coefficient for exponential weighting function	dimensionless
a_1, a_2	coefficients for exponential weighting function	nm^{-1}
C	proportionality coefficient	$(\text{J m}^{-2})^{-1}$
c	principal component scores for each case	dimensionless
$E(\lambda)$	spectral irradiance at wavelength λ	$\text{W m}^{-2} \text{nm}^{-1}$
$E_N(\lambda)$	normalized spectral irradiance at wavelength λ	dimensionless
$\overline{E}_N(\lambda)$	mean normalized spectral irradiance for all treatments	dimensionless
$\text{SD}[E_N(\lambda)]$	standard deviation of $E_N(\lambda)$ for all treatments	dimensionless
E_k	saturation parameter	W m^{-2}
E_{PAR}	PAR irradiance	W m^{-2}
E^*	biologically weighted irradiance	dimensionless
H^*	biologically weighted radiant exposure	dimensionless
i	case number (1 - 72)	dimensionless
Inh	inhibition term	dimensionless
j	wavelength index (1 - 121)	dimensionless
k	principal component number (1 - z)	dimensionless
m_0	coefficient for influence of mean spectrum + PAR	$(\text{J m}^{-2})^{-1}$
m_1, m_2, m_3	coefficients for influence of PCs	$(\text{J m}^{-2})^{-1}$
n	number of treatments (cases)	72
P	rate of photosynthesis	$\text{mg C m}^{-3} \text{h}^{-1}$
P_{avg}	average P	$\text{mg C m}^{-3} \text{h}^{-1}$
P^{B}	P normalized to chlorophyll a	$\text{mg C mg Chl}^{-1} \text{h}^{-1}$
P_{pot}	potential, uninhibited P at irradiance E_{PAR}	$\text{mg C m}^{-3} \text{h}^{-1}$
P_s	maximum potential P for saturating E_{PAR}	$\text{mg C m}^{-3} \text{h}^{-1}$
P_t	P at time t	$\text{mg C m}^{-3} \text{h}^{-1}$
q	number of PCs that are included in curve-fit	dimensionless
t, λ	time	s
T	duration of experiment	s
w	principal component weights for each wavelength	dimensionless
z	number of PCs that describe 99% of spectral variation	dimensionless
\square	biological weighting coefficient	$(\text{W m}^{-2})^{-1}$
$\square_H(\lambda)$	biological weighting coefficient for radiant exposure	$(\text{J m}^{-2})^{-1}$
$\overline{\square}_H$	weighting coefficient for mean spectrum	$(\text{J m}^{-2})^{-1}$
$\square_H(\lambda_r)$	weighting coefficient for reference wavelength	$(\text{J m}^{-2})^{-1}$
$\square_H(\text{PAR})$	weighting coefficient for PAR	$(\text{J m}^{-2})^{-1}$
λ	wavelength	nm
λ_R	reference wavelength	nm

For laboratory cultures at 20°C, we found that inhibition was a function solely of E^* for the time scale considered (0.5 - 4 h).⁴ In contrast to equation A5, the average rate of photosynthesis was well described by an alternate form of equation A6, where $P_{\text{avg}} / P_{\text{pot}} = 1 / (1 + E^*)$, and the BWF was comprised of coefficients $[f(\lambda)]$ with units of reciprocal W m^{-2} .¹⁴

2. Experimental measurements. The analysis requires determinations of P (e.g., from the uptake of ^{14}C -bicarbonate) and spectral irradiance for each treatment. Spectral irradiance, $E(\lambda)$, must be measured accurately for each of the experimental treatments, with good spectral resolution. For our experiments, $E(\lambda)$ is measured from 280 to 400 nm at intervals of 1 nm for each of the 72 treatments, and PAR is measured with a broad-band sensor and compared with measures of spectral irradiance from 400 - 700 nm. It may be impractical to set up such a large number of treatments, but if only a small number of experimental spectra are compared, statistical confidence will suffer.¹

3. Statistical analysis by the Rundel method. For each experiment, 72 values of P over time T are fit to corresponding measurements of E_{PAR} and spectral irradiance according to equation A6, with biologically effective exposure (H^*) quantified (eq. A3) with $f_i(\lambda)$ as an exponential function of wavelength (equation 3). Nonlinear curve-fitting (we use SAS procedure NLIN) is used to determine the photosynthetic parameters P_s and E_k , as well as the coefficients in equation 3 that determine the exponential dependence of biological effectiveness (f_i) on wavelength.

a) We assemble a file with $i = 1$ to 72 cases, each with 123 variables: P_i , E_{PAR_i} and spectra of $E(\lambda)_i$ for 121 wavelengths from 280 - 400 nm. The values are declared as an array, $E(280:400)$. In practice, we normalized $E(\lambda)_i$ to E_{PAR_i} for ease of use with other analyses, but the normalization is not included here.

b) The equation for photosynthesis is:

$$P_i = P_s (1 - e^{-E_{\text{PAR}_i} / E_k}) \cdot \frac{(1 - e^{-H_i^*})}{H_i^*} \quad (\text{A7}).$$

where

$$H_i^* = T \cdot [f_H(\text{PAR}) \cdot E_{\text{PAR}_i}] + \left(\sum_{\lambda=280}^{400} E(\lambda)_i \cdot f_H(\lambda_R) \cdot e^{-(a_1 \cdot (f_H(\lambda) - f_H(\lambda_R)))} \right) \quad (\text{A8}).$$

Unlike Rundel, we assign dimensions to our weighting coefficients, so the weighting for any inhibition due to excess PAR, $f_H(\text{PAR})$, and the weighting at a reference wavelength (we use 290 nm) have units of reciprocal J m^{-2} . For the easier comparison with Rundel's equation (Eq. 3), we

substitute $C \cdot e^{\lambda a_0}$ for the reference weighting, $\int_H(\lambda_R)$; C is a proportionality constant with a value of 1 (J m^{-2})⁻¹:

$$H_i^* = T \cdot [\int_H(\text{PAR}) \cdot E_{\text{PAR}_i}] \cdot \left(\prod_{\lambda=280}^{400} E(\lambda)_i \cdot C \cdot e^{\lambda(a_0 + a_1 \cdot (\int_H(\lambda_R)))} \right) \int_H(\lambda) \quad (\text{A9}).$$

Note that the experimental duration, T , is the same for all treatments. As long as the ERC (Eq. A5) is valid, treatments over different time periods T_i could be included in one analysis.

c) In the program, the parameters P_s , E_k , a_0 , a_1 , and $\int_H(\text{PAR})$ are declared. The model is $P_i = P_{\text{pot}_i} \cdot \text{Inh}_i$, where $P_{\text{pot}_i} = P_s \cdot (1 - e^{-\int_H(\text{PAR}_i) E_k})$. The inhibition term, Inh_i , is $(1 - e^{-H_i^*}) / H_i^*$. It is defined by evaluating equation A9 for each case using a do-loop for $\lambda = 280$ to 400.

d) Estimates for P_s , E_k , a_0 , a_1 , and $\int_H(\text{PAR})$, along with asymptotic standard errors are obtained. Convergence should be faster if derivatives of the parameters are defined and the Marquardt method is used. The procedure can be repeated with the addition of an additional parameter, a_2 , for inclusion in the exponent of equation A9 as $[a_2 \cdot (\lambda - \lambda_0)^2]$. See equation 3. The higher-order term should be included only if it significantly improves the fit, as evaluated with the F -statistic, with 1 and $(n - \text{number of parameters})$ degrees of freedom.

4: Statistical analysis by the PCA method. Here, we use Principal Component Analysis (PCA) to determine statistically-independent spectral shapes that are defined by weights for each wavelength. When scored (i.e., weighted) appropriately for each treatment and combined with the mean spectral shape for the experiment, a small number of principal components (PCs) can reproduce the original spectral shape accurately. The advantage is that a few scores for PCs can provide almost as much information as the original 121 values of $E(\lambda)$ for each spectrum. Consequently, we can use nonlinear curve-fitting to determine the degree to which each PC contributes to the biological effect:^{13,14} if PCs with large weights for shorter wavelengths contribute strongly to the biological effect, the BWF will likewise have strong weighting at short wavelengths, and vice-versa.

a) We start with the same data as for the Rundel method, above. However, because the analysis focuses on spectral shapes, it is necessary to normalize all values of $E(\lambda)$: $E(\lambda)_i$ is multiplied by $\int_H(\lambda)$, the wavelength interval for each spectral estimate (1 nm for this example) and divided by E_{PAR_i} , generating dimensionless values of $E_N(\lambda)_i$. Normalization to $E(400)$ or irradiance at some other wavelength unaffected by the spectral filters would also be suitable.

b) Using the $n = 72$ normalized spectra, compute means and standard deviations for each of the 121 wavelengths: $\overline{E_N(\lambda)}$ and $SD[E_N(\lambda)]$. Save the file for subsequent computations.

c) Conduct a PCA on the normalized spectra using a multivariate statistical analysis package (e.g., SAS), in which the $j = 1$ to 121 variables are $E_N(\lambda)_j$ and the $i = 1$ to 72 cases are the treatments. This PCA is conducted on the correlation matrix. The analysis yields PCs (sometimes called factors), each with 121 component weights (w_j) corresponding to each wavelength, along with information on how much of the aggregate variance in the input spectra is explained by each PC. For each PC, the analysis also yields 72 component scores, c_i , which quantify the contribution of that PC to each treatment spectrum. In our experience, the first few PCs (z ; usually 4) explain >99% of the variance, and only the $k = 1$ to z component scores ($c_{i,k}$) are retained for subsequent analysis. For this example, we will set z to equal 4.

d) Create a data file with 72 cases and 6 variables: P_i , E_{PAR_i} and $c_{i,k}$ for $k = 1$ to z .

e) As before, a nonlinear curve-fitting routine will be used minimize the least-squares error in equation A7, except that here,

$$H_i^* = T \cdot E_{PAR_i} \cdot (m_0 + \sum_{k=1}^z m_k c_{i,k}) \quad (A10).$$

Note that multiplication by T restores the magnitude of each treatment that was removed for the PCA. The coefficient m_0 quantifies the influence of the mean spectrum and a residual weight that represents an irradiance-dependent effect that is not dependent on UV: here, that effect is interpreted as PAR-dependent photoinhibition. The parameters of the model are P_s , E_k , m_0 , m_1 , m_2 , m_3 , and m_4 and the model is $P_i = P_{pot_i} \cdot Inh_i$, where P_{pot_i} is defined as in equation A6, Inh_i is $(1 - e^{-H_i^*}) / H_i^*$; and H_i^* is calculated for each case according to equation A10.

f) The iterative least-squares technique yields estimates for the parameters and their asymptotic errors, along with the amount of variance explained by the model (R^2). The model should be run stepwise for $k = 1$ to z PCs, and each successive component (component q ; $q \leq z$) should be retained only if it significantly increases R^2 (use an F -test with degrees of freedom = 1, n - total number of parameters).

g) The contributions of the PCs, m_i , is transformed back to a spectral weighting, $\overline{w}_i(\lambda)$. For each wavelength:

$$\bar{\Gamma}_H(\lambda) = \frac{\sum_{k=1}^q m_k \cdot w_k(\lambda)}{SD[E_N(\lambda)]} \quad (\text{A11})$$

h) The standard error of $\bar{\Gamma}_H(\lambda)$ is calculated using propagation of the standard errors of the parameters m_i , from the curve-fit analysis. For example, if only two PCs can be statistically justified (i.e., $q = 2$):

$$err[\bar{\Gamma}_H(\lambda)] = \frac{\sqrt{(err(m_1) \cdot w_1)^2 + (err(m_2) \cdot w_2)^2 + 2(r_{1,2} \cdot err(m_1) \cdot w_1 \cdot err(m_2) \cdot w_2)}}{SD[E_N(\lambda)]} \quad (\text{A12})$$

where $r_{1,2}$ is the correlation between m_1 and m_2 from the output of the nonlinear regression analysis. In general for more than two PCs, the standard error is the square root of the matrix product \mathbf{VRV}' divided by $SD[E_N(\lambda)]$, where \mathbf{V} is the vector with elements $[err(m_1 \cdot w_1, m_2 \cdot w_2 \dots)]$ and \mathbf{R} is the correlation matrix of the m 's. That is, if there are 4 PCs in the fit, \mathbf{V} has 4 elements and \mathbf{R} is a 4 x 4 matrix.

Given the standard error of $\bar{\Gamma}_H(\lambda)$, an approximate confidence interval is calculated based on the t statistic with $(n \text{ cases} - \text{total number of parameters})$ degrees of freedom. These are individual (as opposed to joint) confidence intervals for each of the 121 coefficients, i.e., they are not conditioned on the other values of $\bar{\Gamma}_H(\lambda)$. The accuracy of the confidence intervals is dependent on having used the correct underlying model, i.e. equation A6.

i) Once the values for $\bar{\Gamma}_H(\lambda)$ have been calculated, the weighting for the mean treatment spectrum ($\bar{\Gamma}_H$) is evaluated as

$$\bar{\Gamma}_H = \sum_{\lambda=280}^{400} \bar{\Gamma}_H(\lambda) \cdot \bar{E}_N(\lambda) \quad (\text{A13})$$

where the mean normalized spectral irradiance, $\bar{E}_N(\lambda)$ comes from the initial calculation for the analysis (λ is already included in $\bar{E}_N(\lambda)$): see section 4a). Remember that m_0 from the curve-fitting is the contribution of the mean normalized spectrum plus that from PAR: hence the biological weighting coefficient for PAR, $\bar{\Gamma}_H(\text{PAR})$ equals $m_0 - \bar{\Gamma}_H$. Statistical significance of this residual can be assessed by comparison with the standard error of m_0 . We have not evaluated the possible consequences of PAR-inhibition being irradiance-dependent, in part because significant inhibition by PAR has seldom been encountered under our experimental conditions.